MESO-SCALE MODELING OF DAMAGE IN TEXTILE COMPOSITES WITH COMPACTED AND NESTED REINFORCEMENTS

M. Hirsekorn[a*], C. Fagiano[a], A. Doitrand[a], P. Lapeyronnie[a], V. Chiaruttini[a]

[a]*Onera - The French Aerospace Lab, F-92322 Châtillon, France*
**e-mail address of the corresponding author : martin.hirsekorn@onera.fr*

Keywords: Textile Composites, Finite Element Analysis, Damage, Nesting

Abstract
The mechanical behavior of textile composites is modeled at the meso-scale, taking into account the influence of the dry fabric preforming before resin injection, the relative shift and nesting between fabric layers, and the effect of yarn cracking and micro-decohesions at the yarn surfaces. The layer shift has a significant impact on the strain field at the composite surface. If the shifts taken from an experimental specimen are used in the model, the results are in good agreement with those experimentally observed by digital image correlation. The effect of damage is modeled by inserting discrete cracks into the Finite Element model. The numerical results show the same trends as the experimental observations. In order to reach a quantitative agreement, it is necessary to include the effect of micro-decohesions around the crack tips at the yarn surfaces.

1. Introduction

The use of textile composites in industrial applications has been continuously growing throughout the last decade, both in high performance applications (e.g., in the aerospace industry) and in mass production (e.g., in the automotive industry). The main advantages of textile composites include the drapability of the reinforcing fabric on non-developable surfaces and that the reinforcement architecture, and hence the composite properties, can be continuously varied throughout the structure. In addition, complex reinforcement shapes may be woven with the aid of modern looms [1]. These characteristics offer the possibility of reducing the number of parts needed to assemble a composite structure, hence limiting the use of joints, which are classical weak points, and reducing the manufacturing costs.

In recent years, Onera has developed macro-scale models that predict successfully damage evolution and failure in textile composites under quasi-static [2] and fatigue loads [3] However, the parameters of these mainly phenomenological models have to be identified experimentally each time the reinforcement architecture or the constituents change. To exploit efficiently the advantage of varying reinforcements, predictive modeling tools are needed in the design phase, which take into account the reinforcement architecture. This modeling is carried out at a so-called *meso-scale*, a scale that lies in between the *macro-scale* of the structure and the *micro-scale* at which each individual fiber is modeled [4]. At the meso-scale, yarns composed of several thousands of almost parallel fibers are treated as homogeneous material embedded in the matrix. The Representative Unit Cell (RUC) at the meso-scale is a part of the textile reinforcement that entirely represents the reinforcement architecture.

The preforming step consisting of draping and compaction of the fabric is an essential part in the manufacturing process of textile composites. It has a significant influence on the yarn shapes and paths in the final composite and must therefore be taken into account in the meso-scale RUC. In fact, the reinforcement geometry at the meso-scale is very complex, with locally varying fiber volume fraction [5-6], nesting between fabric layers [5,7-8], and complex contact zones between yarns [5-7,9-10]. This influences the local strain distribution in the composite, and hence damage onset and evolution [11-13]. For example, it has been shown [13-16] that the stacking sequence of multi-layer woven composites and the resulting nesting between the layers influence significantly the damage morphology. It is therefore crucial to use yarn shapes as close as possible to reality in meso-scale modeling of textile composites.

There are several automated tools able to generate geometrical models of fabric reinforcements covering a huge variety of weaving patterns [17-19]. However, the yarn deformation occurring during compaction and preforming of the fabric and the nesting between fabric layers is, in most cases, neglected. As a consequence, the resin rich areas between the yarns are bigger than in the real composite, due to the idealized geometrical model [5]. Therefore, in order to preserve the overall fiber volume fraction in the composite (typically 50-60%), the fiber volume fraction in the yarns must be set to very high values (sometimes 90% or higher [20]). Yarn shapes closer to those of the real composite can be obtained from Finite Element (FE) modeling of the dry fabric preforming [9,21-24]. These methods are used in this work to create geometries of a four-layer plain weave fabric with different types of nesting between the layers (Section 2.1). The Finite Element (FE) meshes of the preformed textile RUC including the matrix complement are generated using a recently developed algorithm [25] that ensures conformal meshes at the contact zones between the yarns (Section 2.2).

These meshes are used to compute the local strain fields within the RUC and the influence of the shifts between the fabric layers. In Section 3, the results are compared to strain fields experimentally observed by digital image correlation (DIC) on the surface of a composite specimen made of four layers of plain weave glass fabric embedded in an epoxy matrix. In Section 4, damage is inserted into the RUC in the form of discrete cracks parallel to the fibers within the yarns that are oriented perpendicular to the loading direction, and as decohesions between yarns at the tips of the yarn cracks. This is done using the crack insertion algorithm developed at Onera [26]. The effect of the damage on the homogenized properties of the composite is evaluated by means of FE calculations and are compared to experimental observations on the same specimens. The results of this study provide a basis for the development of a damage model for textile composites that includes the real physics of damage at the different characteristic scales.

2. Generation of a compacted Representative Unit Cell (RUC)

2.1. Modeling of fabric compaction and nesting

A plain weave lay-up with different shifts between adjacent fabric layers is an ideal test case, because it has a relatively simple initial geometry with a small RUC. However, due to compaction and nesting, the yarns are deformed significantly with respect to their initial shape, and multiple contacts between the yarns in each layer and between the layers occur. These effects are taken into account in the FE modeling of the compaction of the fabric RUC without matrix. The initial idealized geometry of a non-deformed layer of plain weave is

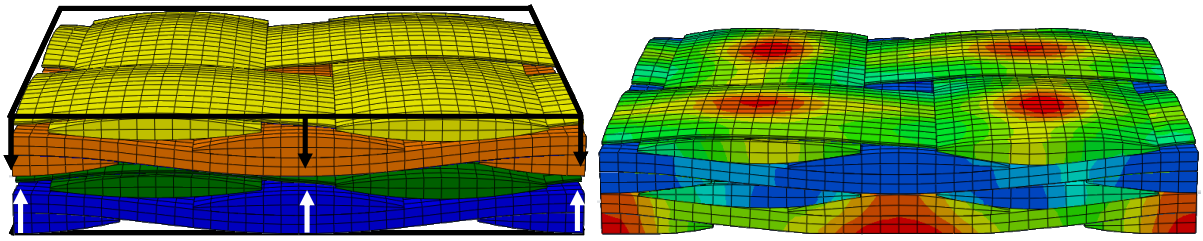

(a) (b)

Figure 1. FE simulation of the compaction of 4 layers of plain weave fabric with maximum nesting. The colors in (b) represent the magnitude of the vertical displacement.

created using the model of Hivet and Boisse [27], also used in [9,21,23] to model dry fabric deformation. Four layers are stacked on top of each other with different in-plane shifts between them. The yarns are extended in both directions of their extremities, using the periodicity conditions of the fabric. They are then cut at the boundaries of the unit cell box, such that each layer is limited to the same unit cell, regardless its position with respect to the adjacent layers. Figure 1a shows the FE mesh of such a lay-up for the case of maximum nesting, which is obtained by shifting adjacent layers by a quarter of the unit cell size both in the direction of the weft and the warp yarns [15]. The dry fabric is then compacted to a final thickness of 1.65mm using the method of Nguyen et al. [23]. A simplified mechanical behavior is used for the yarns [22], which in the case of compaction yields qualitatively good yarn shapes, and is thus adequate to illustrate the procedure. Periodic boundary conditions (BC) are applied to the yarn extremities. The local yarn orientations are obtained by projection on the yarn center line and assigned to each integration point. The result of the compaction modeling is shown in Figure 1b.

The yarn volume fraction (total volume occupied by yarns divided by the total volume of the unit cell) is 52.0% in the initial and 87.3% in the compacted unit cell. Therefore, in order to obtain a total fiber volume fraction in the composite of, e.g., 60%, a typical value for compacted fabrics, the fiber volume fraction in the yarns would have to reach an unphysical value of 115%, if a non-compacted geometry is used as in, e.g., [13,15,28]. The same problem has been encountered by Ivanov et al. [20] for braided fabrics. If the compacted unit cell shown in Figure 1b is used, the fiber volume fraction in the yarns has to be 68.7% in order to reach 60% total fiber volume fraction in the composite, which is quite a realistic value [20].

2.2. Generation of a consistent Finite Element (FE) mesh

FE meshes of yarns of arbitrary shape can easily be generated using automated meshing tools. However, when these yarns come into contact, the surface meshes are, in general, not *conformal*, i.e., the surface nodes are not at the same locations in the contact zone. This is in particular the case for deformed fabrics obtained from modeling the dry fabric preforming, as described in the preceding section, because the yarn surfaces may slide on each other, leading to non-conformal meshes, even if the initial, non-preformed meshes were generated with conformal contact zones. An algorithm has been recently developed at Onera to generate surface meshes of yarns of arbitrary shape that are conformal at the contact zones. It also eliminates small voids and interpenetrations, which are an artifact of any contact modeling between non-conformal meshes. More details to this algorithm can be found in the work of Grail et al. [25]. Figure 2 shows the resulting FE mesh for a compacted lay-up of four layers of plain weave with the layer shifts taken from experimental observations (see next section).

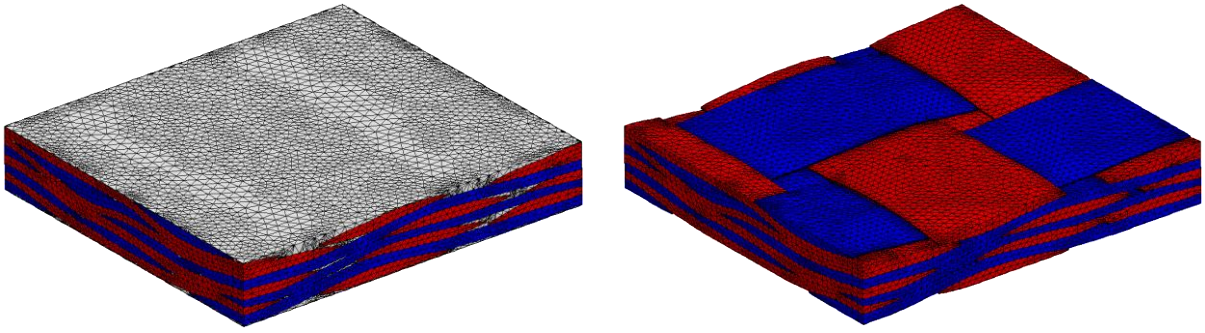

(a) (b)

Figure 2. Optimized FE mesh of the compacted RUC with the experimentally observed shift between the fabric layers. (a) Total RUC with matrix complement. (b) Mesh of the yarns only.

3. Surface strain fields

3.1. Experiments

Composite specimens containing of four layers of an E-glass plain weave fabric in the Araldite LY564 epoxy resin by injection molding have been tested under tension in direction of the warp yarns. In contrast to unidirectional composites, the yarn interlacing pattern in textile composites causes heterogeneous strain fields with large strain gradients around the yarn crimp regions. Classical electrical resistance strain gages can thus not provide an adequate spatial resolution. Therefore, the local strains on the composite surface have been

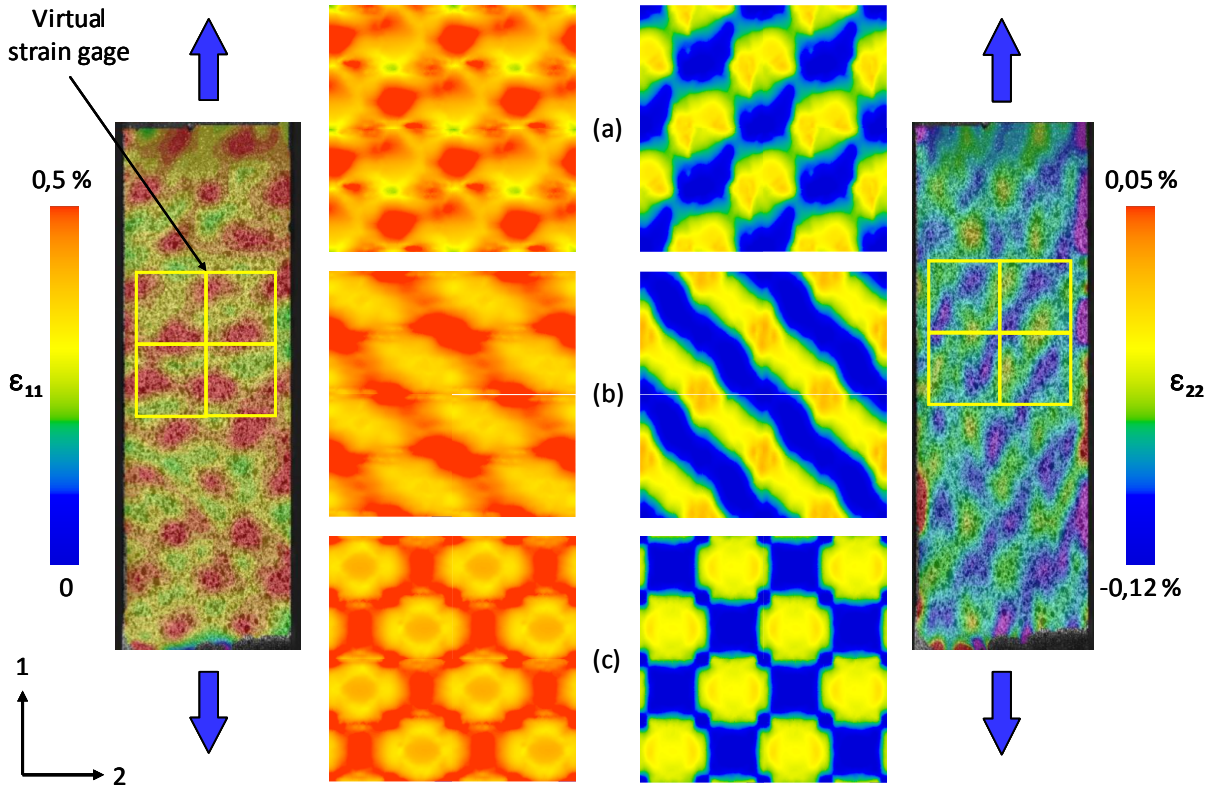

Figure 3. Longitudinal (ε_{11}) and transverse (ε_{22}) strain fields obtained experimentally by digital image correlation on the top surface of a composite specimen with 4 layers of plain weave reinforcement under tensile load in direction of the blue arrows (σ_{11} = 90MPa) compared to FE simulations of four adjacent RUC with different layer shifts: (a) shifts of the specimen, (b) shifts to obtain maximum nesting, and (c) no shifts.

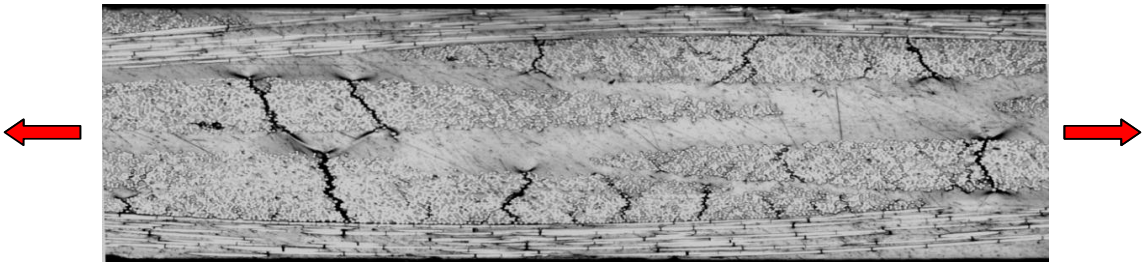

Figure 4. Damage pattern observed by optical microscopy on the specimen edge just before failure (the image was not taken at the failure location).

measured using DIC (see Figure 3). This technique allows for measuring the full strain field including local transverse and shear strain. In addition, damage evolution is monitored by acoustic emission sensors. At different levels of damage, the experiment is stopped, and the elastic properties are measured by averaging over the strain field observed by DIC at low load. The density and total length of the visible cracks on the specimen edge are measured under an optical microscope. The damage just before failure is shown in Figure 4: Transverse yarn cracks are observed with micro-decohesions between yarns and matrix plastification and damage around the crack tips.

3.2. Comparison with numerical simulations

The procedure presented in Section 2 is used to generate FE meshes of a RUC with different shifts between the fabric layers: no shift (and hence no nesting), the layer shift allowing for maximum nesting (see Figure 1), and the layer shifts observed experimentally (see Figure 2). Periodic boundary conditions are applied in the direction of the warp and weft yarns. The top and bottom surfaces are stress free, as in the experiment. The elastic properties of the matrix provided by the manufacturer are E_m = 3.2GPa and ν_m = 0.35. The homogenized transverse isotropic properties of the yarns are obtained from a FE calculation at the micro-scale, as done for example by Melro et al. [28], using E_f = 72.4GPa, ν_f = 0.2 for the E-glass fiber. The fiber orientation at each integration point is obtained by projection on the yarn center line extracted from the compaction modeling. The homogenized elastic properties are calculated from the average stress and strain over the RUC. They agree well with the experimentally measured values and the influence of the layer shift is negligible. The strain fields at the top surface are compared to experimental observations in Figure 3. It can be seen that the local strain distribution is strongly influenced by the shift between the fabric layers. Note that the architecture of the surface layer is the same in all cases, except for an in-plane shift. It is only the relative position of the other layers and the difference in the yarn shapes due to different contacts that cause the different strain patterns. The surface strain fields obtained numerically for in-phase and out-of-phase stacking differ distinctively from those obtained experimentally by digital image correlation. However, if the same relative layer positions as in the studied composite specimen are used to generate the meso-scale composite RUC, the surface strain fields agree very well with the experimental observations, qualitatively (shape of the field) and quantitatively (minimum and maximum values).

4. Influence of damage on the homogenized elastic properties of the composite

4.1. A discrete crack approach to model meso-scale damage

The effect of damage is modeled by inserting cracks into the FE meshes of the RUC using the algorithm of Chiaruttini et al. [26]. This algorithm has been developed to simulate complex

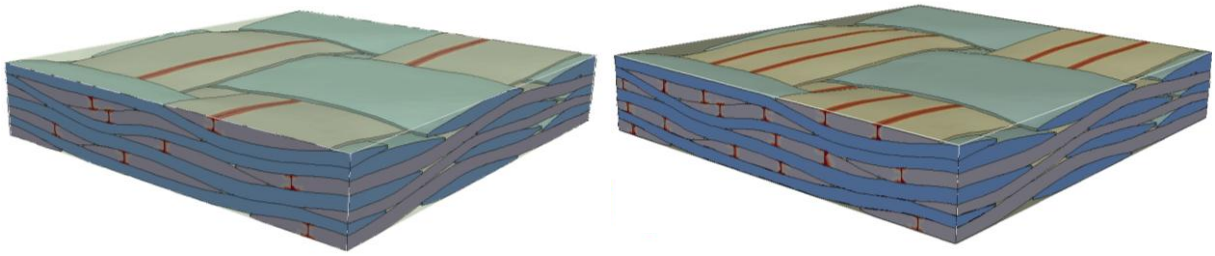

(a) (b)

Figure 5. Representative Unit Cell of four layers of plain weave fabric with transverse cracks in the weft yarns and yarn/yarn and yarn/matrix decohesions around the crack tips: (a) one crack per weft yarn, (b) two cracks per weft yarn.

crack growth phenomena. It is based on the modification of an initially undamaged FE mesh that is refined at the vicinity of the crack front. In a first step, the crack surface geometry is defined by a surface mesh of triangular elements. Then, the undamaged zone of the volume mesh around the crack is adapted such that the crack surface mesh can be inserted. Finally, the volume is remeshed to obtain the RUC with a crack. Zones of micro-decohesion at the yarn surfaces can be automatically generated around the crack tips.

Experimental observations show that at the meso-scale damage starts by cracking of the yarns that are transversely oriented to the load direction (the weft yarns in our case). Decohesion at the yarn surface is observed at the crack tips. To reproduce this kind of damage, we insert transverse yarn cracks one by one into the weft yarns of the RUC mesh, until each weft yarn contains two cracks, located at one third and two thirds of the yarn width (see Figure 5). The cracks are supposed to be oriented perpendicular to the load direction and to run through the whole width of the RUC. Micro-decohesions of different lengths are generated around the crack tips.

4.1. Comparison between numerical simulations and experimental results

The homogenized elastic properties are calculated by FE simulations using the method described in Section 3.2. The decrease of Young's modulus and Poisson ratio with growing crack density is compared to the experimental results in Figure 6. The crack density is the

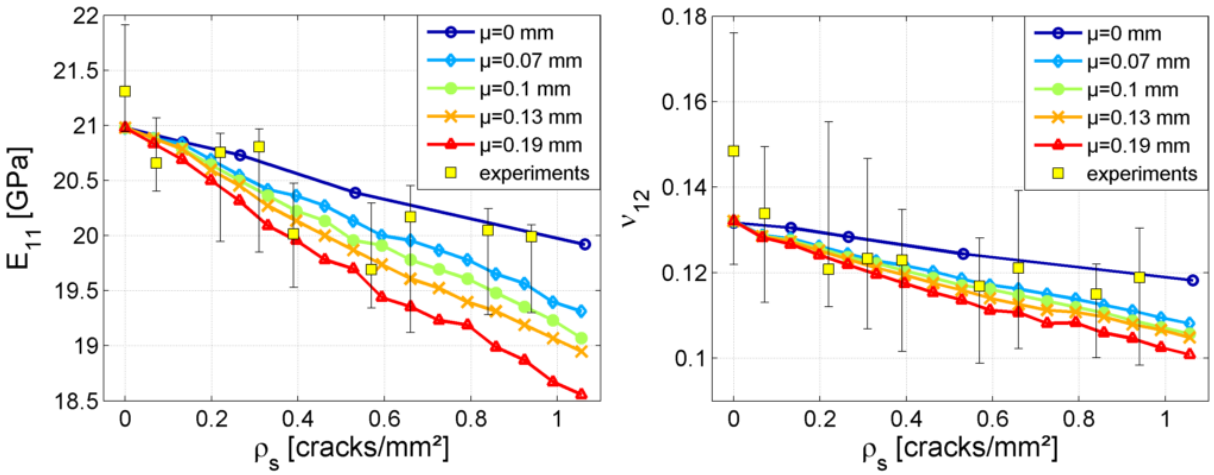

(a) (b)

Figure 6. Comparison between experimental and numerical results of the effect of transverse cracks in the weft yarns on Young's modulus (a) and Poisson ratio (b) in warp direction as function of the crack density ρ_s and the micro-decohesion length μ.

ratio between the number of cracks and the area of the specimen edge, on which the cracks are counted. The results show that the trend of the evolution of Young's modulus and Poisson ratio with the crack density is well predicted by the numerical simulations. The reduction of the properties is slightly underestimated if micro-decohesions are not included. An average decohesion length around the crack tips of 0.1µm gives better results. It has to be noted that in reality not all cracks cover the whole width of the specimen. However, it is impossible to determine their actual length within the specimen without a micro-CT analysis. Such results are not available for the time being, but a study is planned to take place in near future. Therefore, the numerical simulations may overestimate the reduction of the elastic properties, since the total crack surface may be overestimated for a given number of cracks. This leads to the conclusion that the correct micro-decohesion length is probably higher than 0.1µm.

5. Conclusions

A strategy for the numerical simulation of textile composites based on meso-scale FE models of a RUC of the reinforcing fabric has been presented. The influence of dry fabric preforming before resin injection is taken into account by using directly the result of a FE simulation of the fabric compaction in the generation of the FE mesh of the meso-scale RUC. Comparison with strain fields observed by DIC shows that the results are in good agreement with the experiments qualitatively and quantitatively only if the relative shifts and nesting between the fabric layers are correctly included in the model. Damage has been introduced into the FE model by inserting transverse yarn cracks and micro-decohesions at the yarn surfaces around the crack tips. The evolution of the elastic properties obtained from numerical simulations show the same trends as observed by experiments. To obtain a good quantitative agreement in the property reduction due to damage, micro-decohesions around the crack tips have to be included in the model. Despite the simplified crack geometry, the results are encouraging. Future work covers a more detailed modeling of the 3D crack geometry based on micro-CT observations, the inclusion of further damage mechanisms, such as matrix damage and fiber breaking with the aim of predicting the structural behavior of textile composites until failure.

References

[1] A. Mouritz, M. Bannister, P. Falzon, K. Leong. Review of applications for advanced three-dimensional fibre textile composites. *Composites: Part A* 30(12): 1444-1461, 1999.

[2] L. Marcin. *Modélisation du comportement, de l'endommagement et de la rupture de composites à renforts tissés pour le dimensionnement robuste de structures.* Ph.D. Thesis, Université de Bordeaux 1, 2010.

[3] C. Rakotoarisoa, F. Laurin, M. Hirsekorn, J.-F. Maire, L. Olivier. Development of a fatigue model for 3d woven polymer matrix composites based on a damage model. In *Proceedings of ECCM15,* Venice, Italy, 2011, paper 101.

[4] S. V. Lomov, D. S. Ivanov, I. Verpoest, M. Zako, T. Kurashiki, H. Nakai. Meso-FE modelling of textile composites: Road map, data flow and algorithms. *Composites Science and Technology* 67(9):1870-1891, 2007.

[5] M. Olave, A. Vanaerschot, S. V. Lomov, D. Vandepitte. Internal geometry variability of two woven composites and related variability of the stiffness. *Polymer Composites* 33(8):1335-1350, 2012.

[6] M. Karahan, S. V. Lomov, A. E. Bogdanovich, D. Mungalov, I. Verpoest. Internal geometry evaluation of non-crimp 3D orthogonal woven carbon fabric composite. *Composites Part A* 41(9):1301-1311, 2010.

[7] B. Chen, E. J. Lang, T. W. Chou. Experimental and theoretical studies of fabric compaction behavior in resin transfer molding. *Materials Science and Engineering A* 317(1-2):188-196, 2001.

[8] S. V. Lomov, I. Verpoest, T. Peeters, D. Roose, M. Zako. Nesting in textile laminates: geometrical modelling of the laminate. *Composites Science and Technology* 63(7):993-1007, 2003.
[9] P. Badel, E. Vidal-Sallé, E. Maire, P. Boisse. Simulation and tomography analysis of textile composite reinforcement deformation at the mesoscopic scale. *Composites Science and Technology* 68(12):2433-2440, 2008.
[10] J. S. U. Schell, M. Renggli, G. H. van Lenthe, R. Müller, P. Ermanni. Micro-computed tomography determination of glass fibre reinforced polymer meso-structure. *Composites Science and Technology* 66(13):2016-2022, 2006.
[11] S. Daggumati, I. De Baere, W. Van Paepegem, J. Degrieck, J. Xu, S. V. Lomov. Local damage in a 5-harness satin weave composite under static tension: Part I - Experimental analysis. *Composites Science and Technology* 70(13):1926-1933, 2010.
[12] S. John, I. Herszberg, F. Coman. Longitudinal and transverse damage taxonomy in woven composite components. *Composites Part B* 32(8):659-668, 2001.
[13] B. H. Le Page, F. J. Guild, S. L. Ogin, P. A. Smith. Finite element simulation of woven fabric composites. *Composites Part A* 35(7-8):861-872, 2004.
[14] N. V. De Carvalho, S. T. Pinho, P. Robinson. An experimental study of failure initiation and propagation in 2D woven composites under compression. *Composites Science and Technology* 71(10):1316-1325, 2011.
[15] N. V. De Carvalho, S. T. Pinho, P. Robinson. Numerical modelling of woven composites: Biaxial loading. *Composites Part A* 43(8):1326-1337, 2012.
[16] K. Woo, J. D. Whitcomb. Effects of fiber tow misalignment on the engineering properties of plain weave textile composites. *Composite Structures* 37(3-4):343-355, 1997.
[17] I. Verpoest, S. V. Lomov. Virtual textile composites software WiseTex: Integration with micro-mechanical, permeability and structural analysis. *Composites Science and Technology* 65(15-16):2563-2574, 2005.
[18] M. Sherburn. *Geometric and mechanical modelling of textiles*. Ph.D. Thesis, The University of Nottingham, 2007.
[19] G. Couegnat. *Approche multiéchelle du comportement mécanique de matériaux composites à renfort tissé*. Ph.D. Thesis, Université Bordeaux 1, 2008.
[20] D. S. Ivanov, F. Baudry, B. Van Den Broucke, S. V. Lomov, H. Xie, I. Verpoest. Failure analysis of triaxial braided composite. *Composites Science and Technology* 69(9):1372-1380, 2009.
[21] P. Badel, E. Vidal-Sallé, P. Boisse. Computational determination of in-plane shear mechanical behaviour of textile composite reinforcements. *Computational Materials Science* 40(4):439-448, 2007.
[22] L. Hua, M. Sherburn, J. Crookston, A. Long, M. Clifford, I. Jones. Finite element modelling of fabric compression. *Modelling and Simulation in Materials Science and Engineering* 16(3), 2008.
[23] Q. T. Nguyen, E. Vidal-Sallé, P. Boisse, C. H. Park, A. Saouab, J. Bréard. Mesoscopic scale analyses of textile composite reinforcement compaction. *Composites Part B* 44(1):231-241, 2012.
[24] F. Stig, S. Hallström. Spatial modelling of 3D-woven textiles. *Composite Structures* 94(5):1495-1502, 2012.
[25] G. Grail, M. Hirsekorn, A. Wendling, G. Hivet, R. Hambli. Consistent finite element mesh generation for meso-scale modeling of textile composites with preformed and compacted reinforcements. *Composites Part A* 55: 143-151, 2013.
[26] V. Chiaruttini, F. Feyel, J. L. Chaboche. A robust meshing algorithm for complex 3D crack growth simulations. *IV European Conference on Computational Mechanics*, Paris, 2010.
[27] G. Hivet, P. Boisse. Consistent 3D geometrical model of fabric elementary cell. Application to a meshing preprocessor for 3D finite element analysis. *Finite Elements in Analysis and Design* 42(1):25-49, 2005.
[28] A. R. Melro, P. P. Camanho, F. M. Andrade Pires, S. T. Pinho. Numerical simulation of the non-linear deformation of 5-harness satin weaves. *Computational Materials Science* 61:116-126, 2012.